

# CREAM: 70 days of flight from 2 launches in Antarctica

E. S. Seo<sup>a,b</sup>, H. S. Ahn<sup>a</sup>, P. Allison<sup>c</sup>, M.G. Bagliesi<sup>d</sup>, L. Barbier<sup>e</sup>, A. Barrau<sup>f</sup>, R. Bazer-Bachi<sup>g</sup>, J. J. Beatty<sup>c</sup>, G. Bigongiari<sup>d</sup>, P. Boyle<sup>h</sup>, T. J. Brandt<sup>c</sup>, M. Buénerd<sup>f</sup>, J. T. Childers<sup>i</sup>, N. B. Conklin<sup>i</sup>, S. Coutu<sup>j</sup>, L. Derome<sup>f</sup>, M. A. DuVernois<sup>i</sup>, O. Ganel<sup>a</sup>, J. H. Han<sup>a</sup>, J. A. Jeon<sup>k</sup>, K. C. Kim<sup>a</sup>, M. H. Lee<sup>a</sup>, L. Lutz<sup>a</sup>, A. Malinin<sup>a</sup>, M. Mangin-Brinet<sup>f</sup>, P. S. Marrocchesi<sup>d</sup>, P. Maestro<sup>d</sup>, A. Menchaca-Rocha<sup>l</sup>, S. Minnick<sup>m</sup>, S. I. Mognet<sup>j</sup>, S. Nam<sup>k</sup>, S. Nutter<sup>n</sup>, I. H. Park<sup>k</sup>, N. H. Park<sup>k</sup>, A. Putze<sup>f</sup>, R. Sina<sup>a</sup>, S. Swordy<sup>h</sup>, S. Wakely<sup>h</sup>, P. Walpole<sup>a</sup>, J. Wu<sup>a</sup>, J. Yang<sup>k</sup>, Y. S. Yoon<sup>b</sup>, R. Zei<sup>d</sup>, and S. Y. Zinn<sup>a</sup>

<sup>a</sup>*Inst. for Phys. Sci. and Tech., University of Maryland, College Park, MD 20742, USA*

<sup>b</sup>*Dept. of Physics, University of Maryland, College Park, MD 20742, USA*

<sup>c</sup>*Dept. of Physics, Ohio State University, Columbus, Ohio 43210, USA*

<sup>d</sup>*Dept. of Physics, University of Siena and INFN, Via Roma 56, 53100 Siena, Italy*

<sup>e</sup>*NASA Goddard Space Flight Center, Greenbelt, MD 20771, USA*

<sup>f</sup>*Laboratoire de Physique Subatomique et de Cosmologie, Grenoble, France*

<sup>g</sup>*Centre d'Etude Spatiale des Rayonnements, UFR PCA - CNRS - UPR 8002, Toulouse, France*

<sup>h</sup>*Enrico Fermi Institute and Dept. of Physics, University of Chicago, Chicago, IL 60637, USA*

<sup>i</sup>*School of Physics and Astronomy, University of Minnesota, Minneapolis, MN 55455, USA*

<sup>j</sup>*Dept. of Physics, Penn State University, University Park, PA 16802, USA*

<sup>k</sup>*Dept. of Physics, Ewha Womans University, Seoul, 120-750, Republic of Korea*

<sup>l</sup>*Instituto de Fisica, Universidad Nacional Autonoma de Mexico, Mexico*

<sup>m</sup>*Dept. of Physics, Kent State University Tuscarawas, New Philadelphia, OH 44663, USA*

<sup>n</sup>*Dept. of Physics and Geology, Northern Kentucky University, Highland Heights, KY 41099, USA*

## Abstract

The Cosmic Ray Energetics And Mass balloon-borne experiment has been launched twice in Antarctica, first in December 2004 and again in December 2005. It circumnavigated the South Pole three times during the first flight, which set a flight duration record of 42 days. A cumulative duration of 70 days within 13 months was achieved when the second flight completed 28 days during two circumnavigations of the Pole on 13 January 2006. Both the science instrument and support systems functioned extremely well, and a total 117 GB of data including 67 million science events were collected during these two flights. Preliminary analysis indicates that the data extend well above 100 TeV and follow reasonable power laws. The payload recovered from the first flight has been refurbished for the third flight in 2007, where as the payload from the second flight is being refurbished to be ready for the fourth flight in 2008. Each flight will extend the reach of precise cosmic-ray composition measurements to energies not previously possible.

## 1. Introduction

The Cosmic Ray Energetics And Mass (CREAM) experiment (Seo et al., 2004) was designed and constructed to measure cosmic ray elemental spectra using a series of ultra long duration balloon (ULDB) flights. The goal is to extend direct measurements of cosmic-ray composition to the energies capable of generating gigantic air showers which have mainly been observed on the ground, thereby providing calibration for indirect measurements. The instrument has redundant and complementary charge identification and energy measurement systems capable of precise measurements of elemental spectra for  $Z = 1 - 26$  nuclei over the energy range  $\sim 10^{11} - 10^{15}$  eV. Precise measurements of the energy dependence of elemental spectra at the highest of these energies, where the rigidity-dependent supernova acceleration limit could be reflected in a composition change, provide a key to understanding cosmic ray acceleration and propagation.

A relatively large number of measurements of primary cosmic-ray energy spectra have been made with rather good precision at energies up to  $\sim 10^{11}$  eV. Above this energy the uncertainties are large, although there have been some pioneering measurements (Muller et al., 1991; Asakimori et al., 1998; Apanasenko et al., 1999). Whether or not protons have the same spectrum as heavier nuclei is still unclear, especially in view of recent reports from ATIC-1 (Ahn et al., 2006) and ATIC-2 (Wefel et al., 2005). Their different

spectral behavior could be interpreted as evidence for different types of sources/acceleration mechanisms for different elements (Biermann, 1993). A bend in the proton spectrum has been reported to occur near 2 TeV (Grigorov et al., 1971), whereas a different study indicated a bend around 40 TeV (Asakimori et al., 1993). These roll-off energies for protons are 1 - 2 orders of magnitude below the “knee” seen in the all-particle spectrum. An overall trend of flatter high energy spectra for heavy elements was indicated in the data compiled by Wiebel-Sooth et al. (2006) and Horandel (2003).

Secondary cosmic rays produced from the nuclear interactions of primary cosmic rays with the interstellar medium hold a key to understanding the cosmic-ray propagation history. In order to obtain the spectra at the source where cosmic rays are accelerated, the measured spectra must be corrected for propagation effects. Simultaneous measurements of the relative abundances of secondary cosmic rays (e.g. B/C) and the energy spectra of primary nuclei will allow determination of cosmic-ray source spectra at energies where measurements are not currently available.

The instrument was designed to meet the challenging and conflicting requirements to have large enough geometry factor to collect adequate statistics for the low flux of high energy particles, yet stay within the weight limit for space flight. Redundant and complementary detector systems coupled with the ULDB capability being developed by NASA now promise high quality measurements over an energy range that was not previously possible.

## 2. Long Duration Balloon Flights

The CREAM payload was successfully launched from McMurdo, Antarctica on 16 December 2004, and it subsequently circumnavigated the South Pole three times before being terminated on 27 January 2005 (Seo et al., 2005). Both the distance travelled (~14,000 nautical miles) and the time duration (41 days 21 hours 36 minutes) were records for a long duration balloon (LDB) flight. The second launch occurred on 16 December 2005 exactly 1 year after the first launch. That flight circumnavigated the Pole twice before it was terminated on 13 January 2006. A cumulative duration of 70 days within 13 months was achieved when the second flight completed its 28 day journey. As shown by the trajectory of the first flight in Fig. 1a, the balloon drifted toward the Pole, made a tight circle around latitude 85°S, and stayed south of McMurdo for the second circumnavigation, although it gradually spiraled northward. The balloon drifted outward significantly during the third circumnavigation, so the flight was terminated as soon as the balloon came back to the landmass after crossing the water. The payload landed on the high plateau 410 nautical miles northwest of McMurdo station. The recovery crew camped at the landing site to disassemble the

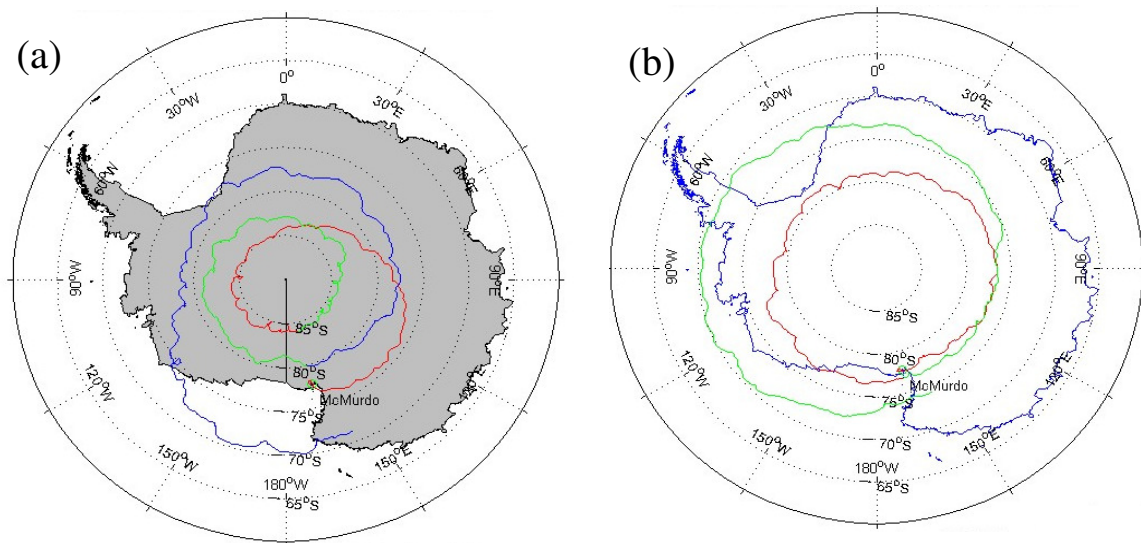


Fig.1. Balloon trajectory of (a) Flight-1 from 16 December 2004 to 27 January 2005, and (b) Flight-2 from 16 December 2005 to 13 January 2006. Both flights were launched from McMurdo. Red curves represent the first circumnavigation, green curves the second, and blue the third circumnavigation.

instrument so it would fit inside the Twin Otter recovery plane. As shown by the trajectory of the second flight in Fig. 1b, the balloon made a larger circle than the first flight. The balloon was visible when it came back to McMurdo after the first circumnavigation. It spiraled out northward and spent a few days over the water during its second circumnavigation. The flight was terminated when it came back to North of McMurdo, and the payload landed 290 nautical miles northwest of McMurdo station. It was much closer than the landing site of the first flight, so its recovery was much easier.

The CREAM flight operation was unique in several aspects: (1) CREAM was the first long duration balloon (LDB) mission to transmit all the prime science and housekeeping data (up to 85 kbps) in near real-time through the Tracking and Data Relay Satellite System (TDRSS) via a high-gain antenna, in addition to having an onboard data archive. To fit the data into this bandwidth, science event records excluded information from channels that had levels consistent with their pedestal value. This 'data sparsification' reduced the average high energy shower event record size by nearly 95%. (2) The instrument was shipped to Antarctica fully integrated to minimize the flight preparation time. The crew made the payload flight ready within 2 weeks after arrival in Antarctica. (3) The science instrument was controlled from the science operation center at the University of Maryland throughout the flight after line-of-sight operations ended at the launch site. Primary command uplink was via TDRSS, with Iridium serving as backup whenever the primary link was unavailable due to schedule or traversing zones of exclusion. The nearly continuous availability of command uplink and data downlink allowed rapid response to changing conditions on the payload (e.g., altitude dependent effects) throughout the flight. See Yoon et al. (2005) and Zinn et al. (2005) for more details about the flight operation and the data acquisition system.

The balloon float altitude was between 125,000 and 130,000 ft (38 and 40 km) throughout most of the flight, as shown in Fig. 2. The corresponding average atmospheric overburden was only  $\sim 3.9 \text{ g/cm}^2$ . The diurnal altitude variation due to the Sun angle change was very small,  $< 1 \text{ km}$ , near the Pole, i.e. at high latitude, although it increased as the balloon spiraled outward to lower latitudes. The temperature of the various instrument boxes stayed within the required operational range with daily variation of a few  $^\circ\text{C}$ , consistent with the Sun angle.

All of the high energy data ( $> \sim 1 \text{ TeV}$ ) were transmitted via TDRSS during the flight, while the lower energy data were recorded on board. A total of 60 GB of data including  $\sim 4 \times 10^7$  science events were collected from the first flight and 57 GB including  $\sim 2.7 \times 10^7$  science events were collected from the second flight.

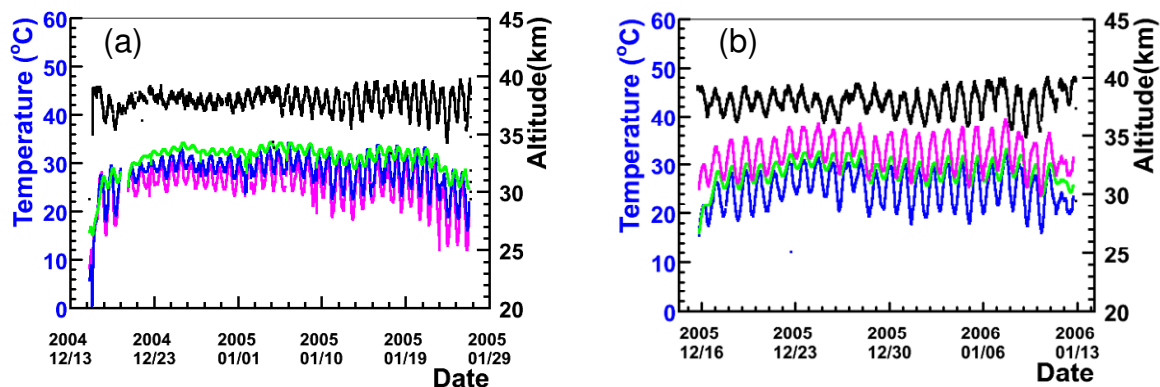


Fig. 2. Altitude of the balloon (black curve) and the temperature of 3 instrument boxes, pink for TCD, green for SCD, and blue for calorimeter, for (a) Flight-1 and (b) Flight-2.

### 3. CREAM Instrument

The CREAM instrument consists of complementary and redundant particle detectors to determine the charge and energy of the high energy particles. They include a Timing Charge Detector (TCD), a Transition Radiation Detector (TRD) with a Cherenkov Detector (CD), and a calorimeter module comprised of a Silicon Charge Detector (SCD), a carbon target, scintillating fiber hodoscopes (S0/S1 and S2), and a stack of tungsten plates with interleaved scintillating fiber layers. A photograph of the CREAM instrument flown on the first flight and a schematic view of the configuration are shown in Fig. 3. See Seo et al. (2004) for

the instrument details. Multiple charge measurements with the TCD, CD, SCD, and S0/S1 layers of scintillating fibers accurately identify the incident particles by minimizing the effect of backscattered particles from the calorimeter. The TCD is based on the fact that the incident particle enters the TCD before developing a shower in the calorimeter, while the backscattered particles arrive several nanoseconds later. A layer of scintillating fibers, S3, located between the carbon target and the tungsten calorimeter provides a reference time. The SCD is segmented into pixels to minimize multiple hits of backscattered particles in a segment.

The carbon target induces hadronic interactions in the calorimeter module, which measures the shower energy and provides tracking information to determine which segment(s) of the charge detectors to use for the charge measurement. Tracking for showers is accomplished by extrapolating each shower axis back to the charge detectors. The hodoscopes S0/S1 and S2 provide additional tracking information above the tungsten stack. Tracking for non-interacting particles in the TRD is achieved with better accuracy (1 mm resolution with 67 cm lever arm, 0.0015 radians). The TRD determines the Lorentz factor for  $Z > 3$  nuclei by measuring transition x-rays using thin-wall gas tubes. The TRD and calorimeter, the latter of which can also measure the energy of protons and He, have different systematic biases in determining particle energy. The use of both instruments allows in-flight cross-calibration of the two techniques and, consequently, provides a powerful method for measuring cosmic-ray energies. As illustrated by the example of a  $\sim 8$  TeV Oxygen event in Fig. 4, the instrument functioned well during the flight. The trigger aperture is  $\sim 2.2$  m<sup>2</sup>sr, and the highly segmented detectors comprising the instrument have about 10,000 electronic channels.

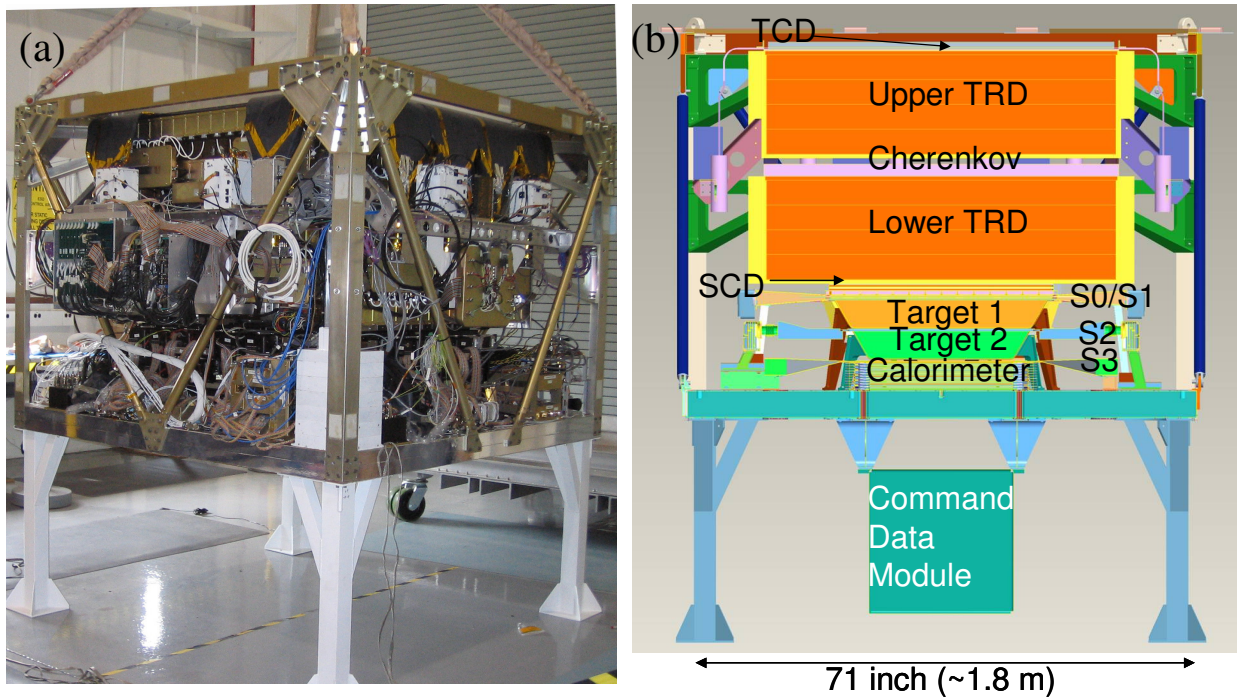


Fig. 3. CREAM Instrument (a) A photograph of the instrument flown on Flight-1, and (b) a schematic view of the instrument configuration.

The CREAM ballooncraft, referring to all hardware below the attachment point to the mobile launch vehicle, shown in Fig. 5, is an integrated assembly of the science instrument and support systems. Unlike most balloon payloads, the science instrument was not pressurized. The main support system was the Command and Data Module (CDM) which was developed by the National Aeronautics and Space Administration (NASA) Wallops Flight Facility (WFF) (Jones et al., 2005). This is in contrast to typical LDB payloads which utilize the Support Instrumentation Package (SIP) provided by the Columbia Scientific Balloon Facility (CSBF). The 40 MCF-lite balloon carried a total suspended weight of 6,000 lb, including  $\sim 2,500$  lb for the science instrument,  $\sim 400$  lb support structure, and  $\sim 1,100$  lb of ballast for the first flight. The suspended weight for the second flight was 5,676 lb including  $\sim 1,200$  lb ballast. The large amount of

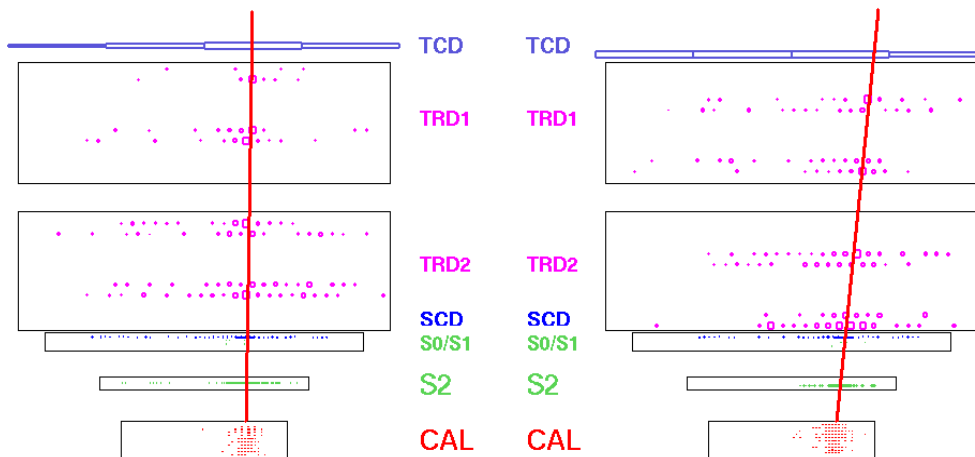


Fig. 4. An example event from the flight data; A cosmic-ray Oxygen nucleus with estimated energy  $\sim 8$  TeV entered the instrument to give a large pulse height (blue box at the top) in the TCD, a clear track in TRD (red squares), a large signal in the SCD (blue squares) and a well-defined shower in the calorimeter (red squares).

ballast played an important role for the zero pressure balloon to keep its high altitude throughout the flight, especially during the third circumnavigation when it drifted northward. The science instrument power consumption was  $\sim 400$  W. Both the science instrument and the flight support systems were developed for nominal 100-day ULDB missions.

The science return depends critically on the exposure factor, since the cosmic-ray flux decreases rapidly as energy increases. The detectors were designed to maximize acceptance of the instrument within the weight constraints for balloon flights. In order to maximize the collecting power, it is desirable to fly as long as possible and as frequently as possible. The instrument and support systems were demonstrated to operate for a long duration during the two already-completed flights. The same instrument cannot be flown in consecutive years due to the time required for recovery, return to the laboratory, and refurbishment, so multiple copies of detectors were (or are being) constructed to take advantage of flight opportunities as frequently as possible.

The performance of the instruments flown on the first two flights can be found elsewhere: TRD/TCD performance (Wakely et al., 2006; Coutu et al., 2005, 2006), Calorimeter performance (Lee et al., 2005; Marrocchesi et al., 2006), SCD performance (Park et al., 2005; Yang et al., 2005; Park et al., 2006).



Fig. 5. CREAM ballooncraft at the launch site, Willams Field in Antarctica, while the balloon is being inflated.

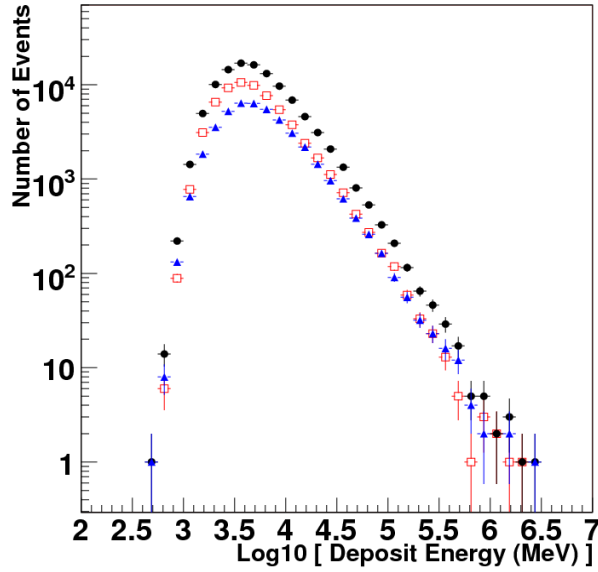


Fig. 6. Preliminary calorimeter energy deposit distribution for Flight-1 (red squares) Flight-2 (blue triangles) and sum of both (black circles).

deposit of about 3.2 along the horizontal scale in Fig. 6 corresponds to incident energy  $\sim 1$  TeV, which is close to the calorimeter threshold. This energy deposit gives a quick check of the energy spectrum, which in this case shows both a reasonable power law and that we have data extending well above 100 TeV. The energy scale is still preliminary with about 10 – 20 % uncertainty. The beam test data taken in various configurations of the calorimeter (i.e., with and without lead bricks in front of and behind the calorimeter module to ensure significant signals at the top and bottom layers), are being compared with Monte Carlo simulations to minimize systematic uncertainties.

The TCD also provided a “ZLO” trigger, which corresponds to light elements below the ZHI threshold. The ZHI threshold was set above He,  $Z > 2$ , for the Flight-1 and above protons,  $Z > 1$ , for Flight-2. The calorimeter energy deposit distributions for the “CAL and ZLO” triggered events are shown with red dashed lines in Figs. 7a and 7b, which correspond to mostly protons and helium for Flight-1 and mostly protons for Flight-2. The calorimeter energy deposit distributions for the “CAL and ZHI” triggered events are shown with blue dotted lines in Figs. 7a and 7b, which correspond to mostly  $Z \geq 3$  for Flight-1 and mostly  $Z \geq 2$  for

#### 4. Data Analysis

The main science event trigger was for high energy particles that deposited significant energy in the Calorimeter (hereafter called the “CAL” trigger), or for heavy nuclei identified from the large pulse height in the TCD (hereafter called the “ZHI” trigger). The CAL trigger was set to require at least 6 consecutive layers with a threshold of  $\sim 60$  MeV. This provided nearly 100% efficiency for showers from protons above 3 TeV (estimated from a Monte Carlo study). Figure 6 shows a preliminary result of the calorimeter energy deposit distribution for events recorded with a CAL trigger for Flight-1 in red squares, Flight-2 in blue triangles, and their sum in black circles. The energy deposit was reconstructed using a preliminary set of calibration constants from a beam calibration, LED-based HV gain corrections, and flight measurements of the ratios between different optical ranges. A

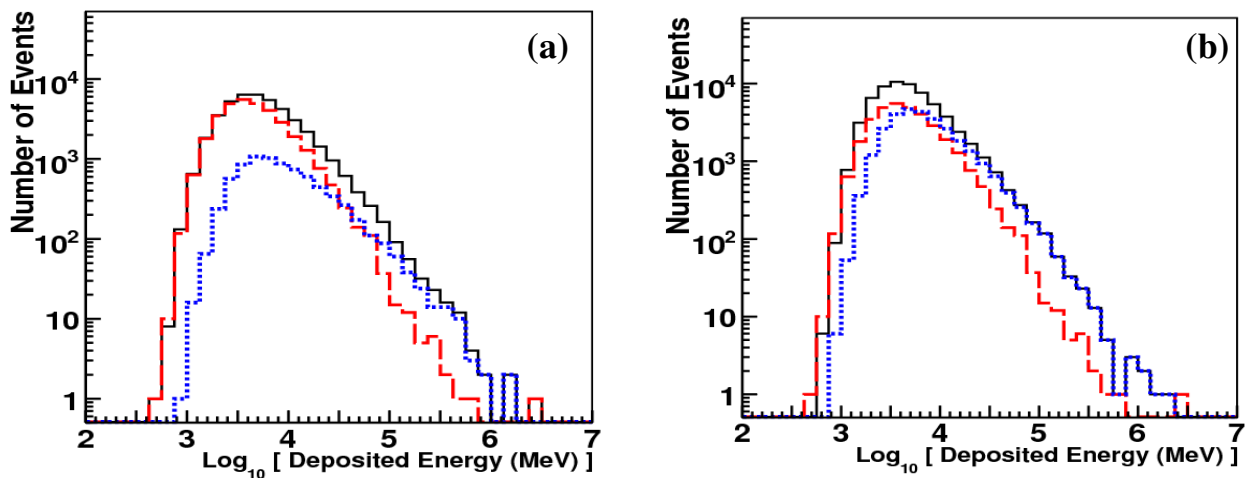


Fig. 7. Comparison of preliminary energy deposit distributions from (a) Flight-1 and (b) Flight-2. Red dashed lines represent “CAL and ZLO” trigger, blue dotted lines represent “CAL+ZHI” trigger, and black solid lines for CAL triggered events.

Flight-2. The CAL triggered events shown with black solid lines in Figs. 7a and 7b have similar steepness (energy dependence) for both flights, implying a consistent all-particle spectrum. The “CAL and ZLO” triggered events are steeper than “CAL and ZHI,” indicating that protons have a steeper spectrum than heavy nuclei. Since the calibration is still in progress, the energy scale is still uncertain. In addition, the events in Fig. 7 include background without proper event selections. Consequently, the power law fits do not accurately represent the spectral indices for either protons or heavy nuclei. Only the qualitative relative difference is meaningful at this stage of the analysis. Nevertheless, this raises interesting questions such as (1) Is the difference due to a steeper proton source spectrum? (2) Are the high energy protons lost preferentially due to an acceleration limit? (3) Is there flattening of heavy nuclei spectra due to weaker energy dependence in the escape length? (4) Is this an artifact due to backscatter, leakage, or something else in the instrument?, etc.? An event reconstruction algorithm to handle backscattered particles, as well as corner-clipping, side-entering, and side-exiting events is being developed, and the related systematic uncertainties are being assessed.

For the charge measurements, analysis of the SCD data begins with tracking information for incident cosmic rays obtained from the TRD and/or the calorimeter. For ZHI triggered events, tracks that are well reconstructed in the TRD are extrapolated to the plane of the SCD. Reconstruction errors in the track angle and offset are considered in defining the search region in the SCD when looking for a matched hit. After subtracting pedestal values, the SCD pixel with the maximum signal in the search area is selected as a candidate. The SCD signal is then corrected for the track angle with respect to the sensor plane. Using the correlation between the reconstructed charge signals from the SCD and the Cherenkov counter, relativistic particles are selected. The resulting SCD charge histogram for ZHI triggered events is shown in Fig. 8. The “CAL and ZLO” triggered events are analyzed similarly by projecting the reconstructed shower axis in the calorimeter to the SCD. The resulting SCD charge histogram for “ZLO and CAL” triggered events is

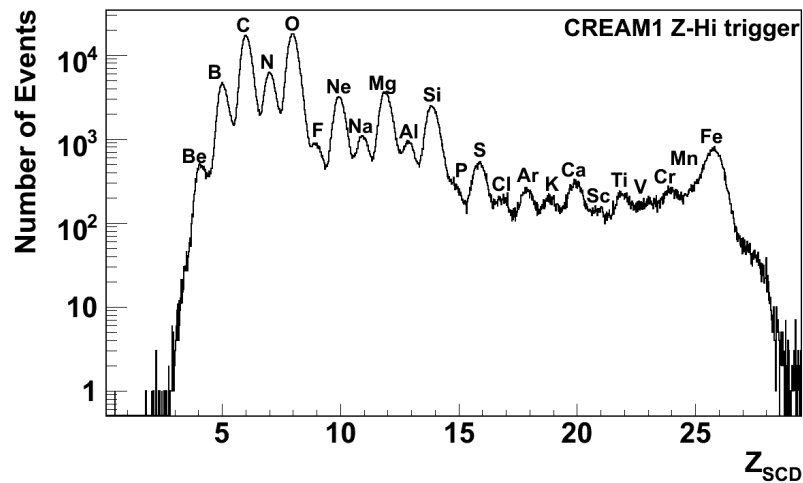


Fig. 8. Preliminary SCD charge histogram for ZHI triggered events.

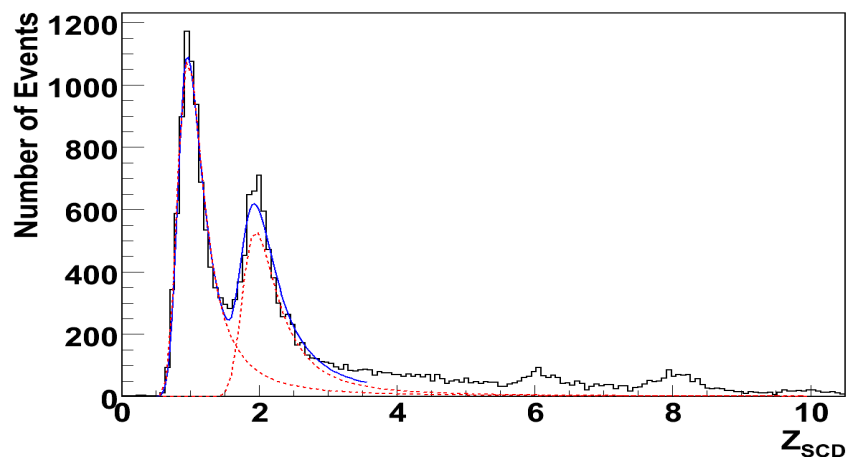


Fig. 9. Preliminary SCD charge histogram for ZLO triggered events.

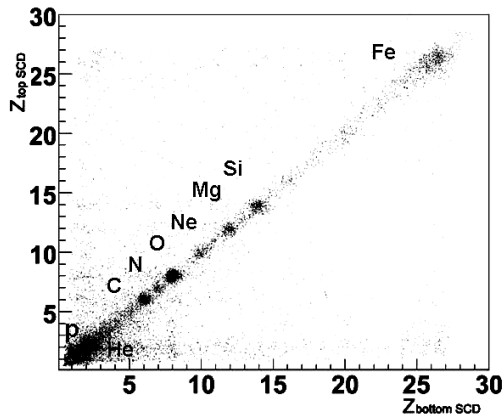


Fig. 10. A scatter plot of top SCD vs. bottom SCD.



Fig. 11. A photograph of glued calorimeter optics including scintillating fiber ribbon, light mixer, and clear fiber bundle being cured in the assembly jig.



Fig. 12. A photograph of the refurbished calorimeter.

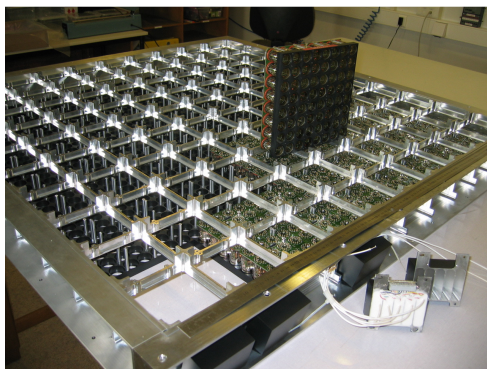


Fig. 13. A photograph of CherCam being assembled for Flight-3.

shown in Fig. 9. Charge peaks for each element from  $Z = 1$  to 28 are clearly separated in the SCD with excellent linearity. Note that the relative abundances shown in these figures are not corrected for detector efficiencies or acceptance.

A major advantage of balloon experiments is that instruments can be improved as flights are repeated. One significant improvement for Flight-2 over Flight-1 is that 2 layers of SCD were used for the Flight-2. Without many corrections, a cross plot of the two independent charge measurements from both layers indicates clear separation of each element, as shown in Fig. 10. Excellent charge resolution can be obtained for Flight-2 by requiring consistency between the two charge measurements. See Marrocchesi, et al. (2006).

## 5. Status Summary

The CREAM instrument landed almost intact after termination of the flight. Even the fragile  $380\mu$  thick silicon sensors were well protected. However, some parts of the instrument had to be cut to go through the Twin Otter recovery plane door. For example, the honeycomb pallet had to be cut into two pieces, the calorimeter optics were destroyed, and some tungsten plates were damaged, etc. The calorimeter optics re-assembly shown in Fig. 11 was one of the major refurbishment efforts. The fully refurbished calorimeter shown in Fig. 12 was calibrated at the CERN SPS in October 2006.

A new addition to the CREAM instrument for Flight-3 is a Cherenkov imager optimized for charge measurements. Figure 13 shows this Cherenkov Camera (CherCam) being assembled. It consists of a silica aerogel Cherenkov radiator plane and a photon detector plane with an array of 1600 1-inch diameter photomultiplier tubes (PMT's). The planes are separated by a 10 cm ring expansion gap to ensure that most Cherenkov photons are collected in 8 tubes surrounding the tube hit by the incident particle. Since upward moving particles will be absorbed in the radiator, the CherCam will provide efficient discrimination against backscattered particles. With CherCam, in addition to the TCD based on timing, and the SCD based on pixellation, the CREAM instrument implements virtually all possible techniques to minimize the effect of backscatter on charge measurements in the presence of the calorimeter. The investigation is striving to achieve charge measurements with the highest possible accuracy.

Another major improvement for Flight-3 will be a redundant Science Flight Computer, which

constituted a potential single point failure for the previous flights. Two computers will be accommodated with a USB interface. New software developed for the USB interface was successfully tested during the 2006 accelerator calibration of the calorimeter. A schematic view of the CREAM ballooncraft configuration for Flight-3 is shown in Fig. 14.

The CREAM instrument was designed and constructed to meet the challenging requirements of ULDB flights of about 100 days. The science instrument, support systems, and operation scheme were successfully tested beyond the nominal 60-day minimum ULDB mission during its first two flights. With excellent particle charge resolution, redundant measurements with complementary detectors, and relatively large collection factor, each CREAM flight will extend the reach of precise cosmic-ray composition measurements to energies not previously possible.

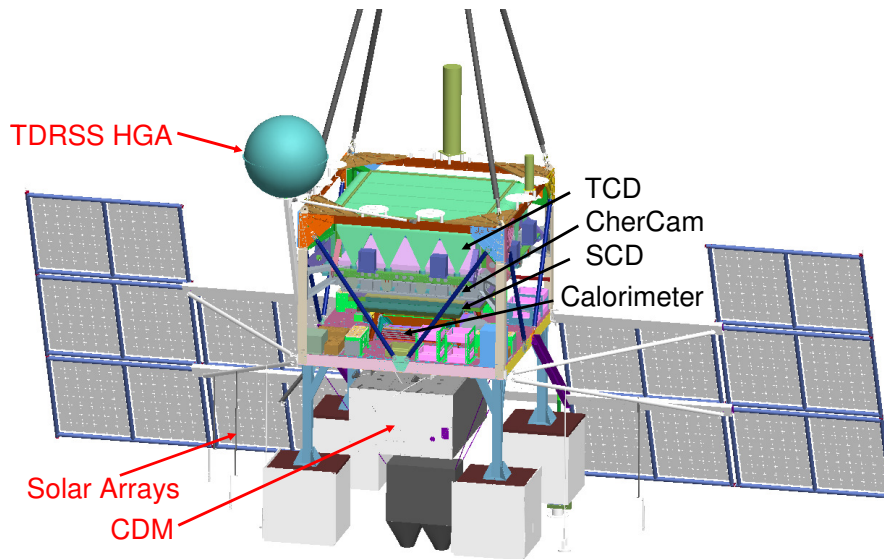


Fig. 14. A schematic view of the CREAM ballooncraft configuration for Flight-3.

#### 4. References

- Ahn, H. S., Seo, E. S., Adams, J. H., et al., The energy spectra of protons and helium measured with the ATIC experiment, *Advances in Space Research*, 37(10), 1950-1954, 2006.
- Apanasenko, A. V., Beresovskaya, V. A., Fujiet, M., et al., Primary cosmic ray spectra observed by RUNJOB, The RUNJOB collaboration, *Proc. 26<sup>th</sup> Int. Cosmic Ray Conf.*, Salt Lake City, 3, 163-166, 1999.
- Asakimori, K., Burnett, T. H., Cherry, M. L., et al., Cosmic ray composition and spectra: (1) Protons, *Proc. 23rd Int. Cosmic Ray Conf.*, Calgary, 2, 21-24, 1993.
- Asakimori, K., Burnett, T. H., Cherry, M. L., et al., Cosmic-ray proton and helium spectra: Results from the JACEE experiment, *Astrophys. Journal*, 502, 278-283, 1998.
- Biermann, P. L., *Cosmic Rays IV: The spectrum and chemical composition above 10<sup>4</sup> GeV*, *Astron. & Astrophys.*, 271, 649-658, 1993.
- Coutu, S., Ahn, H.S., Allison, P. et al., Performance of the transition radiation detector and the timing charge detector in the first flight of the CREAM instrument, *Proc. 29th Int. Cosmic Ray Conf.*, Pune, 3, 393-396, 2005
- Coutu, S., Ahn, H.S., Allison, P. et al., Design and performance in the first flight of the Transition Radiation Detector and Charge Detector of the CREAM balloon instrument, *Proc. of the 10th Pisa Meeting on Advanced Detectors*, in press, 2006.
- Grigorov, N. L., Gubin, Y. V., Jakovlev B. M. et al., Energy spectrum of primary cosmic rays in the 10<sup>11</sup> to 10<sup>15</sup> eV energy range according to the data of Proton-4 measurements, *Proc. 12th Int. Cosmic Ray Conf.*, Tasmania, 5, 1746-1751, 1971.

- Horandel, J. R., On the knee in the energy spectrum of cosmic rays, *Astroparticle Phys.* 19(2), 193-220, 2003.
- Jones, W.V., Pierce, D., Gregory, D. et al., Ultra Long Duration Ballooning Technology Development, *Proc. 29th Int. Cosmic Ray Conf.*, Pune, 3, 405-408, 2005.
- Lee, M. H., Ahn, H. S., Allison, P. et al., Performance of the CREAM calorimeter module during its first flight of 42 days, *Proc. 29th Int. Cosmic Ray Conf.*, Pune, 3, 417-420, 2005
- Marrocchesi, P.S., Ahn, H.S., Allison, P. et al., Preliminary results from the second flight of CREAM, *Adv. in Space Res.*, submitted, 2006.
- Müller, D., S. P. Swordy, P. Meyer et al., Energy spectra and composition of primary cosmic rays, *Astrophys. J.*, 374, 356-365, 1991.
- Park, I. H., Ahn, H.S., Allison, P. et al., The first flight measurement with the CREAM Silicon Charge Detector, *Proc. 29th Int. Cosmic Ray Conf.*, Pune, 3, 341-344, 2005.
- Park, N. H. Ahn, H.S., Allison, P. et al., The First Flight of the CREAM Silicon Charge Detector, *J. of Korean Physical Society.* 49(2), 815-818, 2006.
- Seo E. S., Ahn, H. S., Beatty, J. J. et al., Cosmic Ray Energetics And Mass (CREAM) balloon project, *Adv. in Space Res.*, 33/10, 1777-1785, 2004; <http://cosmicray.umd.edu/cream/cream.html>.
- Seo, E. S., Ahn, H. S., Allison, P. et al., New observations with CREAM, *Proc. 29th Int. Cosmic Ray Conf.*, Pune, 10, 185-198, 2005.
- Wakely, S. P., Ahn, H. S., Allison, P. et al., First measurements of cosmic-ray nuclei at high energy with CREAM, *Adv. in Space Res.*, submitted, 2006.
- Wefel, J.P., Adams, J.H., Ahn, H.S., et al., Energy spectra of H and He from the ATIC-2 experiment, *Proc. 29th Int. Cosmic Ray Conf.*, Pune, 3, 105-108, 2005.
- Wiebel-Sooth, B., Biermann, P. L., Meyer, H., Cosmic Rays VII. Individual element spectra: prediction and data, *Astron. & Astrophys.*, in press, 2006.
- Yang, J., Ahn, H.S., Allison, P. et al., Performance of the CREAM Silicon Charge Detector during its first flight, *Proc. 29th Int. Cosmic Ray Conf.*, Pune, 3, 345-348, 2005.
- Yoon, Y. S., Ahn, H.S., Allison, P., et al., Flight operations during the first CREAM Balloon Flight, *Proc. 29th Int. Cosmic Ray Conf.*, Pune, 3, 429-432, 2005.
- Zinn, S.Y., Ahn, H.S., Allison, P., et al. The data acquisition software system of the 2004/2005 CREAM experiment, *Proc. 29th Int. Cosmic Ray Conf.*, Pune, 3, 437-440, 2005.

## 5. Acknowledgements

This work is supported by NASA grants in the US, by the Korean Ministry of Science and Technology in Korea, by INFN in Italy, and by IN2P3 in France. The authors thank NASA/WFF, Columbia Scientific Balloon Facility, National Science Foundation Office of Polar Programs, and Raytheon Polar Service Company for the successful balloon launch, flight operations, and payload recovery.

## 6. Figure Captions

- Fig. 1. Balloon trajectory of (a) Flight-1 from 16 December 2004 to 27 January 2005, and (b) Flight-2 from 16 December 2005 to 13 January 2006. Both flights were launched from McMurdo. Red curves represent the first circumnavigation, green curves the second, and blue the third circumnavigation.
- Fig. 2. Altitude of the balloon (black curve) and the temperature of 3 instrument boxes, pink for TCD, green for SCD, and blue for calorimeter, for (a) Flight-1 and (b) Flight-2.
- Fig. 3. CREAM Instrument (a) A photograph of the instrument flown on Flight-1, and (b) a schematic view of the instrument configuration.
- Fig. 4. An example event from the flight data; A cosmic-ray Oxygen nucleus with estimated energy  $\sim 8$  TeV entered the instrument to give a large pulse height (light blue box at the top) in the TCD, a clear track in TRD (red squares), a large signal in the SCD (blue box) and a well-defined shower in the calorimeter (red squares).

- Fig. 5. CREAM ballooncraft at the launch site, Willams Field in Antarctica, while the balloon is being inflated.
- Fig. 6. Preliminary calorimeter energy deposit distribution for Flight-1 (red squares) Flight-2 (blue triangles) and sum of both (black circles).
- Fig. 7. Comparison of preliminary energy deposit distributions from (a) Flight-1 and (b) Flight-2. Red dashed lines represent “CAL and ZLO” trigger, blue dotted lines represent “CAL+ZHI” trigger, and black solid lines for CAL triggered events.
- Fig. 8. Preliminary SCD charge histogram for ZHI triggered events.
- Fig. 9. Preliminary SCD charge histogram for ZLO triggered events.
- Fig. 10. A scatter plot of top SCD vs. bottom SCD.
- Fig. 11. A photograph of glued calorimeter optics including scintillating fiber ribbon, light mixer, and clear fiber bundle being cured in the assembly jig.
- Fig. 12. A photograph of the refurbished calorimeter.
- Fig. 13. A photograph of CherCam being assembled for Flight-3.
- Fig. 14. A schematic view of the CREAM ballooncraft configuration for Flight-3.